Piezoelectricity in wurtzite

nextnano++ and nextnano^3 can simulate growth orientation dependence of the piezoelectric effect in heterostructures. Following A.E. Romanov *et al*., Journal of Applied Physics **100**, 023522 (2006), we consider $In_xGa_{1-x}N$ and $Al_xGa_{1-x}N$ thin layers pseudomorphically grown on GaN substrates. The c-axis of the substrate GaN is inclined by an angle θ with respect to the interface of the heterostructure. The layer is assumed to be very thin compared to substrate so that the strain is approximately homogeneous in all direction (pseudomorphic), and the ternary alloys mimic the orientation of crystallography direction. The layer material deforms such that the lattice translation vector of each layer has a common projection onto the interface. The strain in a crystal induces piezoelectric polarization, which contributes as an additional component to the total charge density profile. The important consequence of their analysis is that the piezoelectric polarization normal to the interface **becomes zero at a nontrivial angle**. The piezoelectric charge in a heterostructure in general results in an additional offset between electron and hole spatial probability distribution, thereby reducing the overlap of their wavefunctions in real space. The small overlap of electron and hole leads to an inefficient radiative recombination, i.e. lower efficiency of optoelectronic devices. The work by Romanov *et al*. paved the way to device optimization by the growth direction of the crystal.

References

- A.E. Romanov *et al*., Journal of Applied Physics **100**, 023522 (2006)
- S. Schulz and O. Marquardt, Phys. Rev. Appl. **3**, 064020 (2015)
- S.K. Patra and S. Schulz, Phys. Rev. B **96**, 155307 (2017)

The corresponding input files are:

- Romanov_InGaN_theta_nnp.in
- Romanov_AlGaN_theta_nnp.in
- Romanov_InGaN_theta_nnp_2nd.in
- Romanov_InGaN_theta_nn3.in
- Romanov_InGaN_theta_nn3_2nd.in

Specify crystal orientation

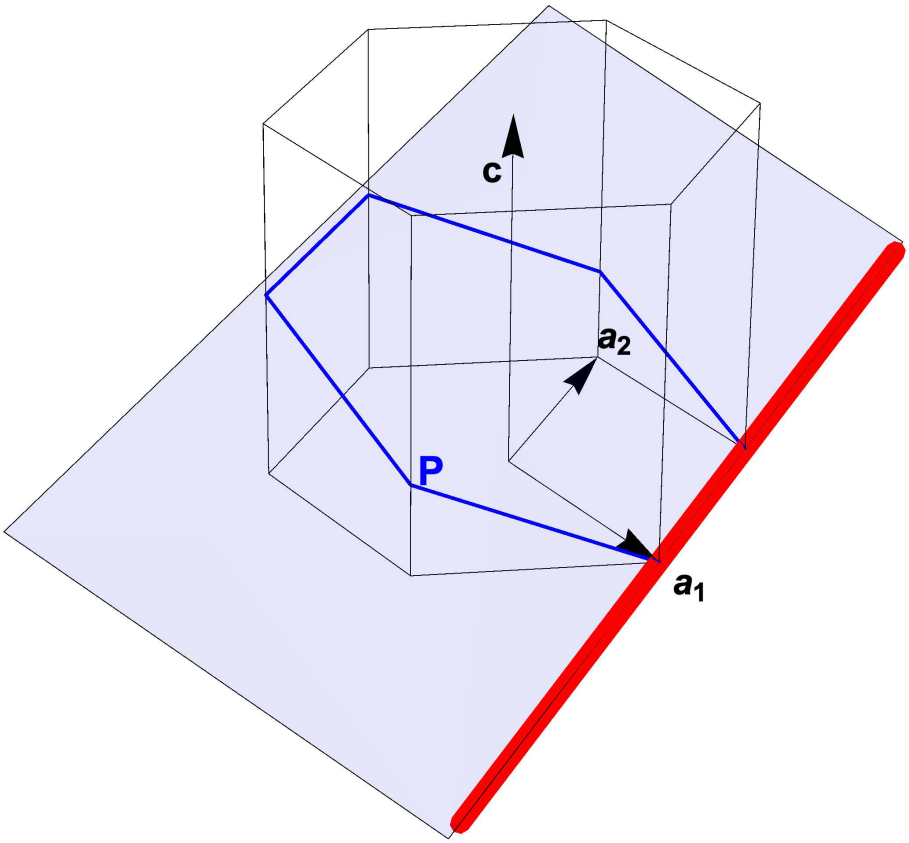

Figure 1: Rotation of a wurtzite structure. The blue plane is parallel to the interface.

nextnano software treats the rotation of crystal orientation by the **Miller-Bravais indices** in the input file. The setup of our system is as follows: the x-axis of the simulation coordinate system (hereafter **x'**-axis) is taken to the normal vector of the interface. The z-axis of the simulation system (**z'**) is normal to the (-1 2 -1 0) plane of the crystal, i.e. it is along $\mathbf{a}_2$ direction in Figure 1. The rotation axis indicated with red line is along **z'**-axis, and the interface is shown as the blue plane. The inclination angle θ is defined as the angle between the c-axis [0001] and the normal vector of the blue plane, which is **x'**-axis. Then the crystal orientation is specified in nextnano++ input file as

```
crystal_wz{
     x_hkl = [ 1, 0, l(theta)] # x axis perpendicular to (hkl) plane =
(hkil) plane
     z_hkl = [-1, 2, 0]        # z axis perpendicular to (hkl) plane =
(hkil) plane
}
```

where $l(\theta)$ is an integer determined by the inclination angle. This statement means *the **x'**-axis is normal to the (1 0 -1 $l(\theta)$) plane of the crystal, whereas **z'**-axis is normal to the (-1 2 -1 0) plane*. (Note that nextnano++ does not require the third entry, i.e. the letter `i`, in Miller-Bravais notation (hkil) because `i=-(h+k)`.)

The index $l(\theta)$ is deduced from a simple geometry consideration. Figure 2 shows the cross-section of a wurtzite lattice that is perpendicular to the rotation axis in Figure 1.

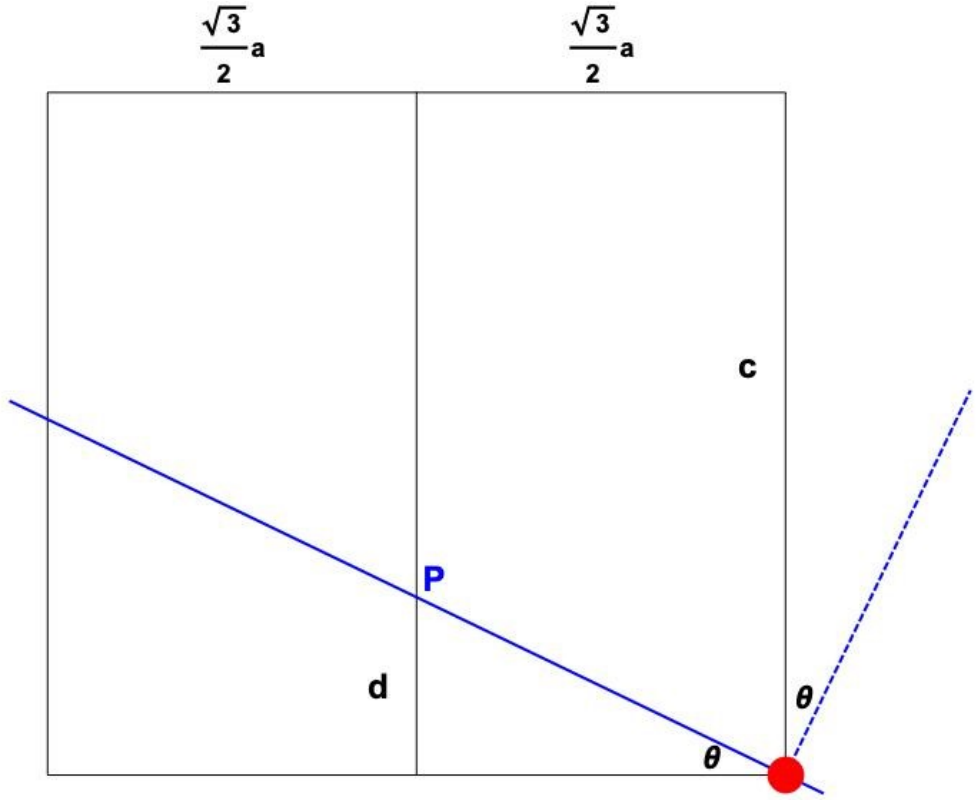

Figure 2: Cross-section of the wurtzite lattice. The dashed blue line indicates the **x'**-direction, which is normal to the interface (solid blue line).

- When $\theta=0$, the interface is normal to the (0001) plane, i.e. **x'**-axis is normal to the (0001) plane.
- When $\theta=90$ degree, the **x'**-axis should be normal to the (1 0 -1 0) plane of the crystal.
- When $0<\theta<90$ degree, definition of the index is $l(\theta):= \frac{c}{d}$ and the following relation holds $$d=\frac{\sqrt{3}}{2}a\tan{\theta}.$$ From these equations we find $$l(\theta)=\frac{2c}{\sqrt{3}a\tan{\theta}}.$$ The plane to be determined can be then taken as $$(hkil) = (\sin\theta\ \ 0\ \ -\sin\theta\ \ \frac{2c}{\sqrt{3}a}\cos\theta).$$

We note that the expression in the third case includes the other two special cases. To approximate the direction with integer entries, we multiply 100 and take the floor function:

```
$h = floor(100*sin(theta))
$k = floor(100*2c*cos(theta)/sqrt(3)a)
x_hkl = [$h, 0, $l]  # x axis perpendicular to (hkl) plane = (hkil) plane
```

Since nextnano[3] does not support variables in the Miller-Bravais indices, we explicitly give the indices in the input file using statements like `!IF %ORIENTATION40 hkil-x-direction = 64 0 -64 143`.

Parameter sweep of the angle using Template: Sweep over the variable theta

- Input file: Romanov_InGaN_theta_nnp.in

One can make use of '**Template**' feature of nextnanomat to sweep the angle θ and obtain crystal orientation dependence of several physical quantities. Here, calculation is performed for every 5 degrees (Figure 3).

Figure 3: 'Template' tab in nextnanomat.

We obtain the angle dependence using '**Postprocessing**' feature. Here, we collect the strain tensor components ε_{xx}, ε_{yy}, ε_{zz}, ε_{xy}, ε_{xz} and ε_{yz} that are in columns 2, 3, 4, 5, 6, 7 of the file `strain_simulation.dat`.

- Select file containing values for the strain tensor components `strain_simulation.dat` by clicking on the folder icon below *Postprocessing*.
- Select 1 for the *Maximum number of values lines*.
- Select 2 for the *Number of relevant column*. *(to do: Improve nextnanomat to include all columns.)*
- Click on *Create file with combined data* to generate file `theta_strain_simulation_Column2.dat`.
- Select 3 for the *Number of relevant column*.
- Click on *Create file with combined data* to generate file `theta_strain_simulation_Column3.dat`.
- Select 4 for the *Number of relevant column*.
- Click on *Create file with combined data* to generate file `theta_strain_simulation_Column4.dat`.
- Select 5 for the *Number of relevant column*.
- Click on *Create file with combined data* to generate file `theta_strain_simulation_Column5.dat`.
- Select 6 for the *Number of relevant column*.
- Click on *Create file with combined data* to generate file `theta_strain_simulation_Column6.dat`.
- The postprocessing results are contained in the folder `<name_of_input_file>_postprocessing`.
- Finally, the plotted results of the postprocessing file can be exported to gnuplot. Add all columns to the Overlay, and then click on: *Create and Open Gnuplot (*.plt) from Items of Overlay*

Strain

Figures 4 and 5 are the strain tensor elements as a function of inclination angle θ, with respect to **simulation** and **crystal** coordinate systems, respectively. One can confirm that they reproduce correctly Figure 5 and 6 in [Romanov2006]. Please note that Romanov takes **z'**-axis as growth direction, while we take **x'**-axis. Therefore **x'**- and **z'**-axes are interchanged from [Romanov2006].

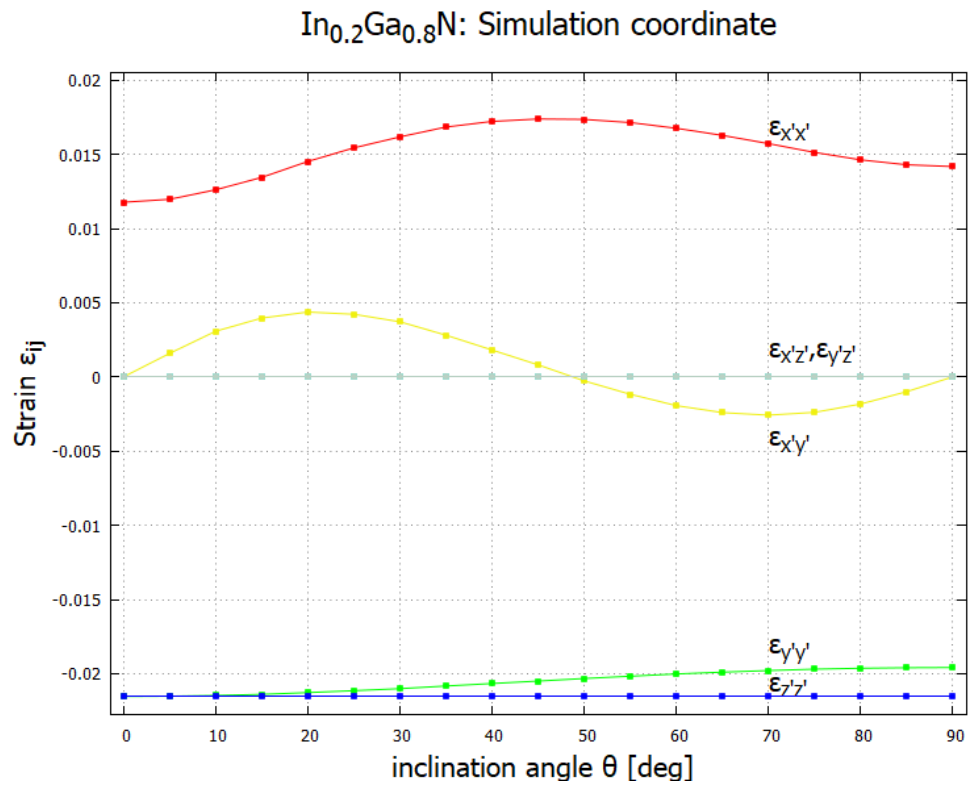

Figure 4: Elastic strain tensor components as a function of c-axis inclination angle θ in **simulation** coordinate system.

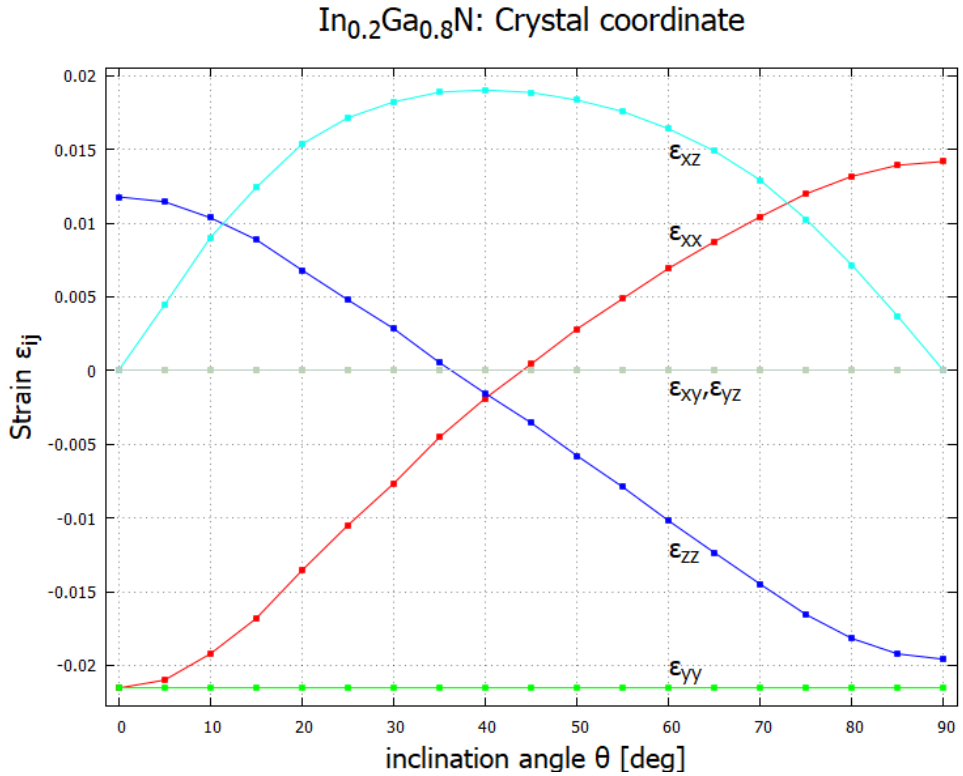

Figure 5: Elastic strain tensor componentsas a function of c-axis inclination angle θ in **crystal** coordinate system.

Piezoelectric effect (first-order)

The piezoelectric effect is at first instance described by a linear response against strain. In crystal coordinate system, $$ P_\mu^{(1)}=\sum_{j=1}^6 e_{\mu j}\epsilon_j, $$ where $\mu=1,2,3$ and the strain tensor is expressed in six-dimensional Voigt notation $$ \begin{pmatrix} \epsilon_{1} \\

\epsilon_{2} \\ \epsilon_{3} \\ \epsilon_{4} \\ \epsilon_{5} \\ \epsilon_{6} \end{pmatrix} =\begin{pmatrix} \epsilon_{xx} \\ \epsilon_{yy} \\ \epsilon_{zz} \\ 2\epsilon_{yz} \\ 2\epsilon_{xz} \\ 2\epsilon_{xy} \end{pmatrix}. $$ Please note that the indices x, y, z without prime refer to the axes of the crystal coordinate system. The superscript $^{(1)}$ indicates first-order piezoeffect. For the symmetry of the wurtzite structure, only three parameters remain in the piezoelectric coefficient tensor e_{ij} $$ \begin{pmatrix} P_x^{(1)} \\ P_y^{(1)} \\ P_z^{(1)} \\ \end{pmatrix} = \begin{pmatrix} 0 & 0 & 0 & 0 & e_{15} & 0 \\ 0 & 0 & 0 & e_{15} & 0 & 0 \\ e_{31} & e_{31} & e_{33} & 0 & 0 & 0 \end{pmatrix} \begin{pmatrix} \epsilon_{xx} \\ \epsilon_{yy} \\ \epsilon_{zz} \\ 2\epsilon_{yz} \\ 2\epsilon_{xz} \\ 2\epsilon_{xy} \end{pmatrix} = \begin{pmatrix}2e_{15}\epsilon_{xz} \\ 2e_{15}\epsilon_{yz} \\ e_{31}(\epsilon_{xx}+\epsilon_{yy})+e_{33}\epsilon_{zz} \end{pmatrix}, $$ cf. Eq. (4) in [Schulz2015]. **Note that Eq. (14) in [Romanov2006] misses the factor 2 for off-diagonal elements of the strain tensor, i.e. $P_x^{(1)}$ and $P_x^{(1)}$ have to be corrected by a factor of 2.**

These equations are implemented in both the nextnano++ and nextnano^3 software with corresponding material parameters in the respective database. The following flags export the strain tensor components and piezoelectric polarization vector in **crystal** and **simulation** coordinate systems (cf. nextnano++ and nextnano3 documentation). The piezoelectric polarization vector with respect to the simulation coordinate system can be found in the file `Strain\piezoelectric_polarization_vector_simulation.dat`.

```
# nextnano++
strain{
   output_strain_tensor{
      crystal_system    = yes
      simulation_system = yes
   }
   output_polarization_vector{
      crystal_system    = yes
      simulation_system = yes
   }
}
```

```
! nextnano3
$output-strain
   strain-simulation-system = yes
   strain-crystal-system    = yes
   polarization-vector      = yes
$end_output-strain
```

For consistency, we have used the same material parameters as [Romanov2006], i.e. we have overwritten our default material parameters of the database with the values specified in the input file.

Analytical expression is derived as follows [Schulz2015]. Since we are interested in the polarization normal to the interface, it is useful to switch to the simulation coordinate system (x', y', z'). This can be done by transforming the polarization vector and the strain tensor to the simulation system, $$ P_{\mu'}^{(1)}=\sum_{\mu=1}^3 R_{\mu'\mu} P_\mu^{(1)},\ \ \epsilon_{\mu'\nu'}=\sum_{\mu,\nu=1}^3 R_{\mu'\mu}R_{\nu'\nu}\epsilon_{\mu\nu}, $$ where the 3×3 rotation matrix R accounts for a rotation of angle θ. Prime denotes the axes in

simulation coordinate system. The second transformation is given in Eq. (13) in [Romanov2006]. The second equation can be expressed in the six-dimensional notation as $$ \epsilon_{i}=\sum_{j'=1}^6 S_{ij'}\epsilon_{j'}, $$ where S is a 6×6 matrix, whose elements depend on θ. The piezoelectric polarization vector in the simulation coordinate system is therefore given as $$ \begin{pmatrix} P_{x'}^{(1)} \\ P_{y'}^{(1)} \\ P_{z'}^{(1)} \end{pmatrix} =R(\theta) \begin{pmatrix} 0 & 0 & 0 & 0 & e_{15} & 0 \\ 0 & 0 & 0 & e_{15} & 0 & 0 \\ e_{31} & e_{31} & e_{33} & 0 & 0 & 0 \end{pmatrix} S(\theta) \begin{pmatrix} \epsilon_{x'x'} \\ \epsilon_{y'y'} \\ \epsilon_{z'z'} \\ 2\epsilon_{y'z'} \\ 2\epsilon_{x'z'} \\ 2\epsilon_{x'y'} \end{pmatrix}. $$ The **z'**-component is explicitly $$ P_{z'}^{(1)}= e_{31}\cos\theta\epsilon_{x'x'}\\ +\left(e_{31}\cos^3\theta+\frac{e_{33}-2e_{15}}{2}\sin\theta\sin 2\theta \right) \epsilon_{y'y'} \\ +\left(\frac{e_{31}+2e_{15}}{2}\sin\theta\sin 2\theta+e_{33}\cos^3\theta \right) \epsilon_{z'z'} \\ +\left[(e_{31}-e_{33})\cos\theta\sin 2\theta+2e_{15}\sin\theta\cos 2\theta\right] \epsilon_{y'z'}. $$ **Note that the corresponding analytical expression Eq. (18) in [Romanov2006] misses the factor 2 in front of e_{15} in the 2nd, 3rd and 4th line, and contains a typo in the 3rd line, i.e. it must be e_{31} and not e_{33} in the first term of the 3rd line.** Figure 6 compares the results of the nextnano software with the results of [Romanov2006] and [Schulz2015], respectively. The analytical results in Figure 6 are the plot of this equation, with an interchange of **x'**- and **z'**-axes.

Figure 6: Piezoelectric polarization as a function of inclination angle. The gray curve is the analytical result of Eq. (18) in [Romanov2006], i.e. the curve (4) in Fig. 7(a) where the factor 2 is missing.

From the result we can see that the piezoelectric polarization vanishes at an intermediate angle around 38 degree, and that it is maximized when inclination angle is zero.

Alloy content dependence

One can also sweep the alloy content x. The following result corresponds to Figure 7(a) in [Romanov2006]. One can see that the zero point is universal for different alloy content.

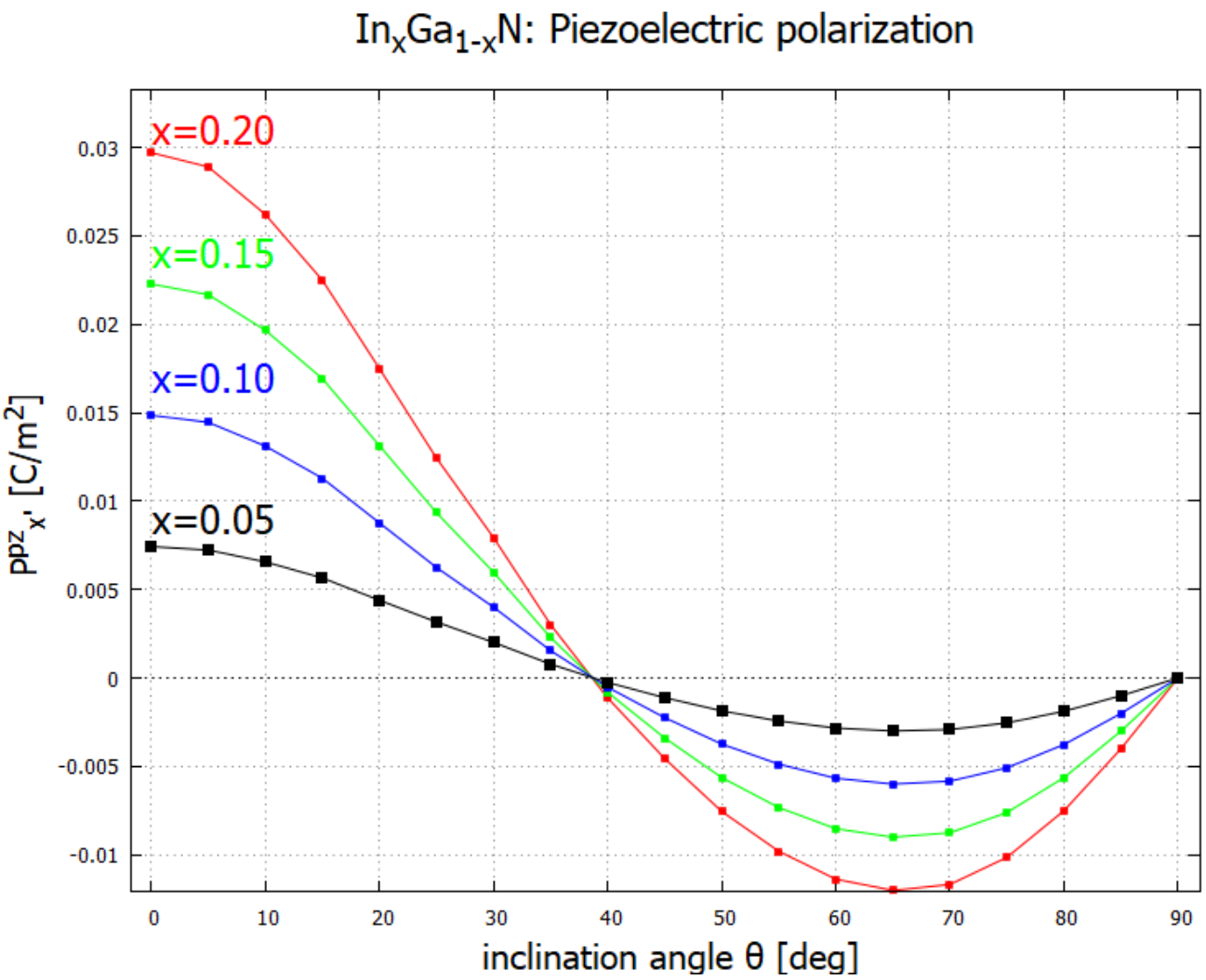

n
ce of the piezoelectric polarization.

AlGaN

- Input file: Romanov_AlGaN_theta_nnp.in

Similarly, piezoelectric polarization of Al$_x$Ga$_{1-x}$N/GaN structure is calculated and shown in Figure 8. This result corresponds to Figure 8(a) in [Romanov2006]. The piezoelectric effect vanishes at around 38 degree in this case as well.

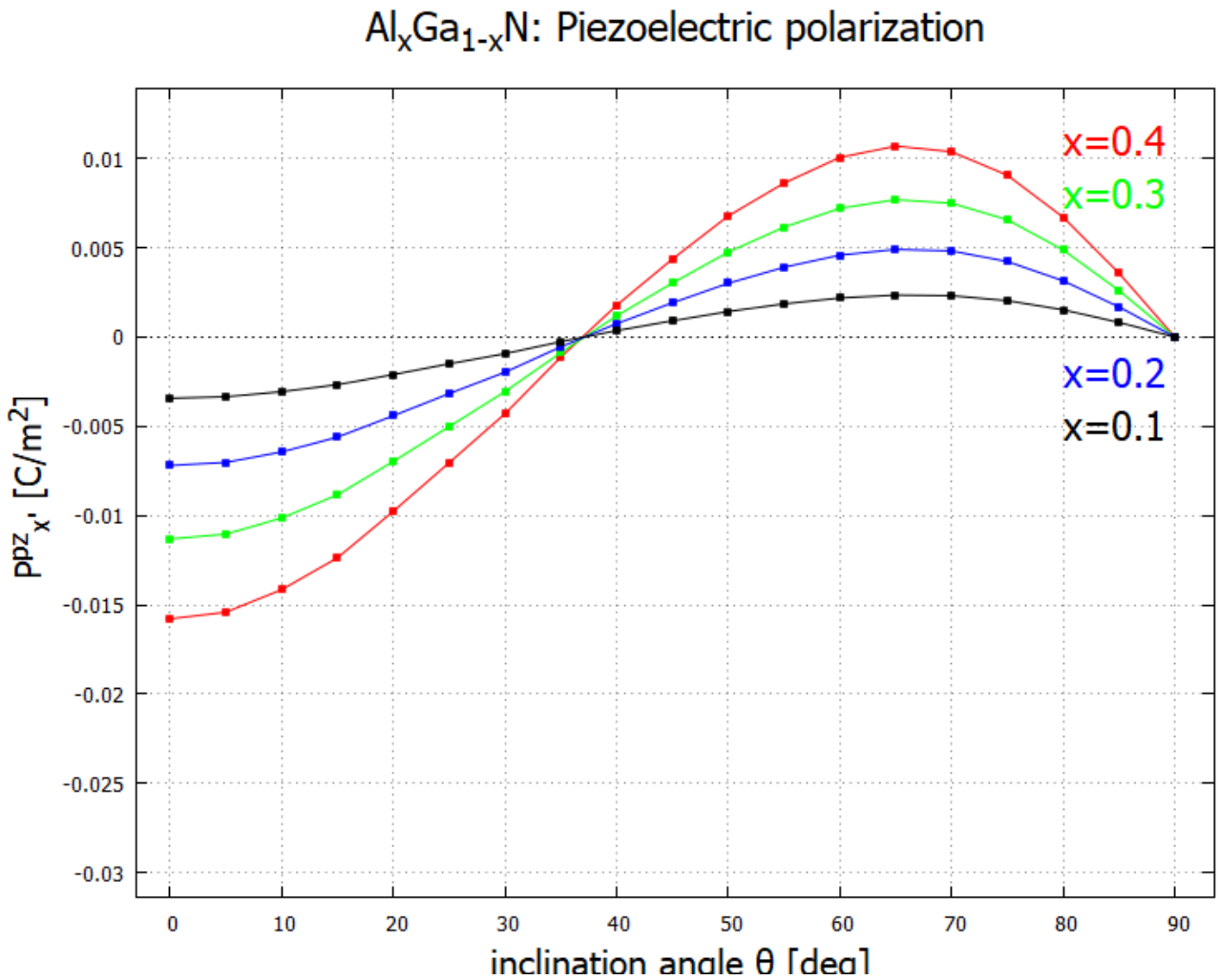

e
nce of the piezoelectric polarization for $Al_xGa_{1-x}N$/GaN structure.

Piezoelectric effect (second-order)

- Input file: Romanov_InGaN_theta_nnp_2nd.in

Optimization of optoelectronic device design requires an accurate and detailed knowledge of the growth-direction dependence of the built-in electric field. Recently, the second order piezoelectric effect has been reported to be relevant for wurtzite III-N materials, namely GaN, AlN and InN. This potentially affects the electronic and optical properties of the devices. The piezoelectric polarization is generalized in crystal coordinate as [Patra2017] $$ P_\mu^{\mathrm{pz}}=\sum_{j=1}^6e_{\mu j}\epsilon_j+\frac{1}{2}\sum_{j,k=1}^6 B_{\mu jk}\epsilon_j\epsilon_k+\cdots $$ where $e_{\mu j}$ and $B_{\mu jk}$ are first- and second-order piezoelectric coefficients, respectively. For binary wurtzite structure, one can show that $B_{\mu jk}$ has 8 independent components $B_{311}, B_{312}, B_{313}, B_{333}, B_{115}, B_{125}, B_{135}, B_{344}$. The explicit expression of the second-order term is given in Eq. (3) in [Patra2017], which is also implemented in nextnano++.

One can turn on the second-order contribution in nextnano++ as

```
# nextnano++
strain{
   ...
   second_order_piezo = yes        # default: no
```

```
}
```

and in nextnano3

```
! nextnano3
$numeric-control
   ...
   piezo-second-order = 2nd-order    ! [no/2nd-order/2nd-order-Tse-Pal]
$end_numeric-control
```

Figure 9 shows the result of nextnano software. While the second-order contribution becomes negligible between the orientation $(1 0 \bar{1} 3)$ and $(1 0 \bar{1} 2)$, it enhances the piezo effect up to 14% in other directions. This figure can be qualitatively compared to Figure 1 (c) in [Patra2017], but note that they consider binary InN/GaN structure there. The pink curve is different from the one in Figure 6 because we employed the material parameters used in [Patra2017]. nextnano^3 yields slightly deviated result, as it uses different formula for the second-order effect, L. Pedesseau et al., Appl. Phys. Lett. 100, 031903 (2012). Also see nextnano3 documentation.

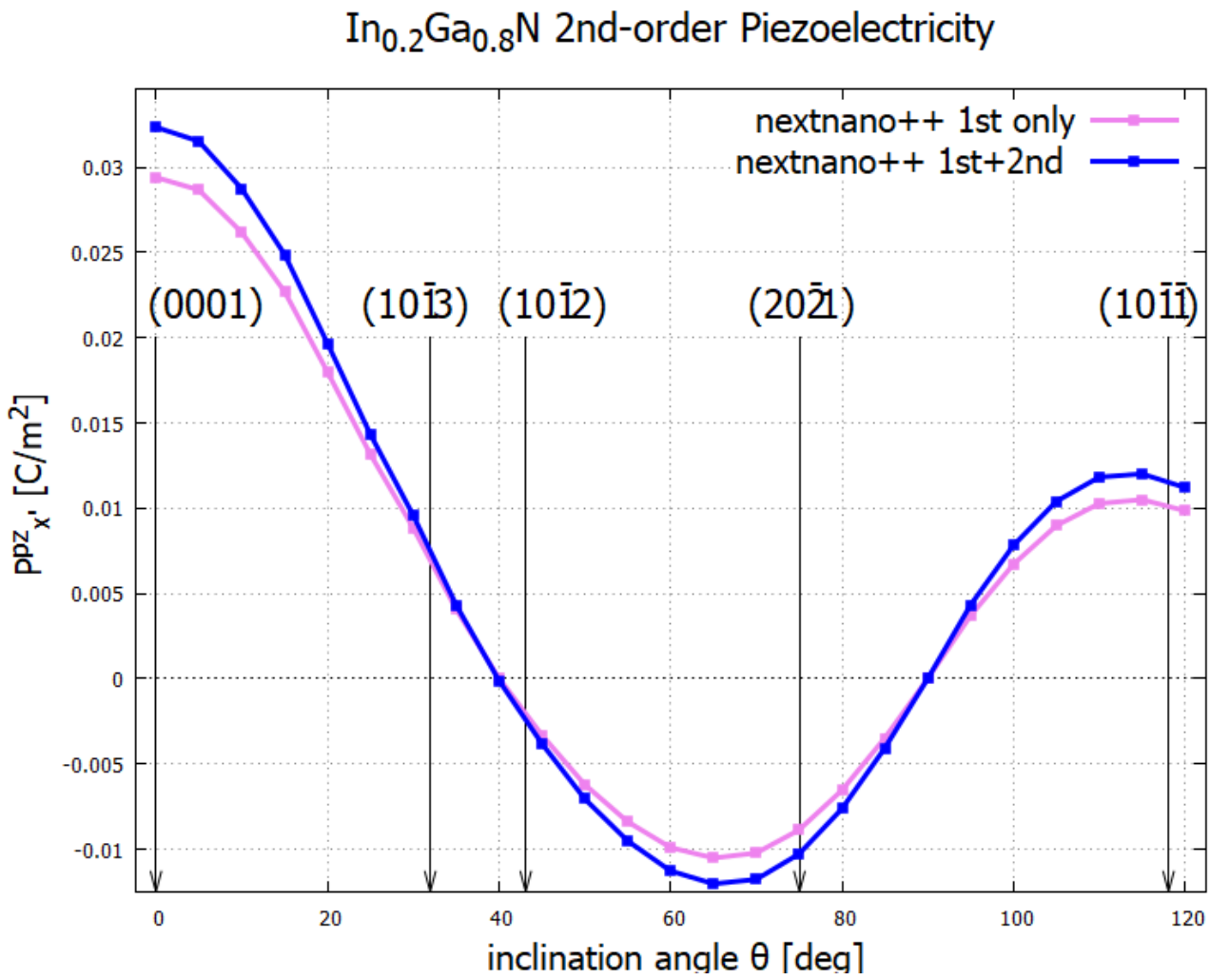

l

ectricity. Interface planes are indicated at corresponding angles.

- Please help us to improve our tutorial! Should you have any questions and comments, please contact to support [at] nextnano.com.